

IAC-19, E2, 4,7, x53582

## Solar Panel Deployment Mechanism for a Solar Sailing Nanosatellite

Vaibhav B. Wanere<sup>a</sup>,

Mr Rohit Patil<sup>b</sup>, Mr Juber Shaikh<sup>c</sup>, Ms Chaitra Shet<sup>d</sup>, Ms Tanaya Bapat<sup>e</sup>, Mr Roven Pinto<sup>f</sup>, Ms Mansi Kabade<sup>g</sup>, Mr Pravin Londhe<sup>h</sup>, Mr Akshay Deodhar<sup>i</sup>

<sup>a</sup>College of Engineering Pune, India, wanerevb17.mech@coep.ac.in

<sup>b</sup>College of Engineering Pune, India, rohitshambhu@gmail.com

<sup>c</sup>College of Engineering, Pune, India, shaikhj17.mech@coep.ac.in

<sup>d</sup>College of Engineering, Pune, India, shetcs18.mech@coep.ac.in

<sup>e</sup>College of Engineering, Pune, India, bapattd18.mech@coep.ac.in

<sup>f</sup>College of Engineering, Pune, India, pintor15.mech@coep.ac.in

<sup>g</sup>College of Engineering Pune, India, kabademm15.mech@coep.ac.in

<sup>h</sup>College of Engineering Pune, India, londheps15.mech@coep.ac.in

<sup>i</sup>College of Engineering Pune, India, deodharar17.mech@coep.ac.in

### Abstract

Solar cells are used in satellites to satisfy the power demand. In case of solar sailing missions, the sunlight falls only on a limited portion of the satellite due to the presence of the large solar sail and hence the solar cells attached to the satellite walls may not satisfy the power requirements. To increase the number of solar cells facing the sun, deployable solar panels with solar cells fixed on them are needed. These panels are kept in a stowed state using a nylon wire before launch owing to the constrained volume availability in the launch vehicle. This paper is about the design and testing of a reliable, minimum power-consuming solar panel deployment mechanism for COEPSAT-2 which is a nanosatellite being developed by the students of College of Engineering, Pune (COEP). The satellite aims to demonstrate orbit manoeuvring using a solar sail of area 40 meter-square while characterizing the charged particle density in space. The satellite has four solar panels with nine solar cells on each panel. The mechanism uses an outside stop type hinge, loaded with a 180-degree torsion spring of stiffness 1.5 N-mm/degree. One leaf of the hinge is fixed on the satellite while the other movable leaf holds the solar panel. The working of the mechanism consists of three stages viz. release, deployment, and locking. When the nylon nichrome mechanism is actuated the panel gets deployed by the torsion spring. The locking is done after deployment using a cam follower mechanism in which the follower fixed on the free end of a flat spring moves into a slot made on the cam integral with the movable leaf. Due to the geometry of the mechanism, there is a definite relationship between the upward movement of the follower block and rotation of the panel. Constraints on the length, allowable deflection of the free end of the flat spring and the need of sufficient locking force demanded material for flat spring with high Young's modulus and high tensile strength which led to the selection of carbon fiber. Design of the hinge, torsion spring and hinge pin was done using analytical calculations and structural simulations. The mechanism was successfully tested experimentally by deploying the panels horizontally to minimize the effect of gravity. Thus this paper provides the design and validation of an effective method of deployment and locking of the solar panels for a solar sailing nanosatellite.

**Keywords:** Solar Sailing Missions, Solar Cells, Deployable Panels, Torsion Spring, Cam-Follower, Flat Spring, Locking

### Nomenclature

1.  $I$  - Mass moment of inertia of the solar panel
2.  $m_{panel}$  - Mass of the solar panel
3.  $l_{panel}$  - Length of solar panel
4.  $t$  - time required for deployment
5.  $k_t$  - Stiffness of the torsion spring
6.  $\theta$  - Angular displacement of solar panel from the deployed position
7.  $\theta_0$  - Angular displacement of solar panel in un-deployed position
8.  $\ddot{\theta}$  - Angular acceleration of the solar panel
9.  $T_f$  - Frictional torque opposing the deployment
10.  $\mu$  - Coefficient of friction for ABS plastic
11.  $F_N$  - Normal force exerted by the flat spring on cam in un-deployed position
12.  $D$  - mean coil diameter of torsion spring

13.  $d$ - wire diameter of torsion spring
14.  $N$ - Number of active coils of torsion spring
15.  $R_{cam}$ - radius of cam
16.  $E_{torsion}$ - Modulus of elasticity of torsion spring material
17.  $E_{flat\ spring}$ - Modulus of elasticity of flat spring material
18.  $C$ - Spring index
19.  $r$ - The number of half cycles after which a vibrating system comes to rest

#### Acronyms/Abbreviations

**COEP:** College of Engineering Pune

**CSAT:** COEP Satellite

**SPD:** Solar Panel Deployment

**CFRP:** Carbon Fibre Reinforced Plastic

**ADCS:** Attitude Determination and Control System

#### 1. Introduction

After a successful launch of the first passively stabilised Indian satellite Swayam (COEPSAT-1), the team CSAT is now working on its next solar sailing satellite mission COEPSAT-2 which aims to demonstrate orbit raising using solar sails and characterise the charged particles in space during its lifetime. There are two options to provide a CubeSat with electrical energy: solar cells attached to the body of the satellite and solar cells attached to a planar structure able to be deployed; called as solar panels [1]. COEPSAT-2 being a solar sailing mission, the solar sails present don't allow the sunlight to reach the side faces (sat body) of the satellite and on the other hand even in case of non-solar sailing missions when the satellite is in space all the cells attached to different faces of the satellite are not exposed to the sunlight which may lead to an insufficient power generation for the mission. This problem has been dealt with by increasing the number of cells facing the sun which necessitated the use of the deployable solar panels for the satellite.

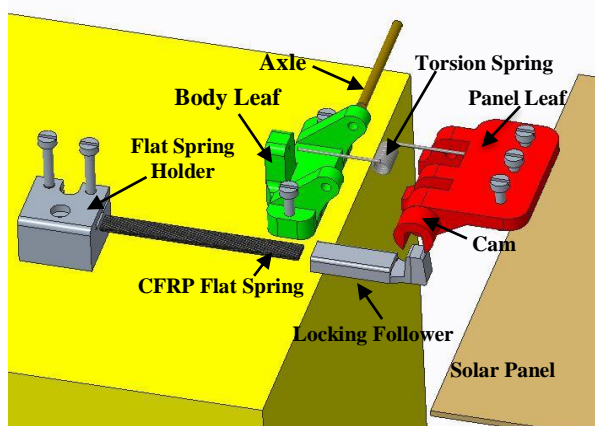


Fig.1 Exploded view of the mechanism

A broad classification of solar panel deployment systems can be performed based on the deployment geometry and solar panel's orientation once deployed [6]. Three categories have been determined based on this classification: (i) the deployment involves single solar panels, which are connected to the satellite body by one single hinge; (ii) the deployment involves a number of solar panels connected in a chain and one solar panel is connected to the satellite body by one single hinge, without the possibility of steering the solar array once deployed; (iii) the deployment involves one or more solar panels connected in a chain and one solar panel is connected to the satellite body by a system of two hinges, allowing to rotate the solar panel system relative to the satellite body once the solar panel is deployed [6]. The work presented in this paper has been limited to case (i) from the above listed.

The solar panels can be deployed using the active as well as passive mechanisms. Active mechanisms require power resources to turn on mechanical elements generating deployment motions, usually through electric motors. Passive techniques do not require any electrical power resources, so they contemplate, for instance, the use of mechanical springs to provide the necessary energy for deployment [1]. Owing to the limited power availability; design, manufacturing and implementation complexity of the active means, the COEPSAT-2 is employing passive means for deployment as well as locking. Some of the most used passive mechanisms for nanosatellites are those based on coil springs, torsion springs and flexible joints (tape springs) [1]. Torsion spring and tape spring have been found suitable and have been compared in table 1 for various parameters which led to the selection of torsion spring for the mechanism due to its design and manufacturing flexibility.

Table 1. Comparison between Torsion Spring and Tape Spring [1], [8].

| Sr. No. | Parameter  | Torsion Spring | Tape Spring                   |
|---------|--|----------------|-------------------------------|
| 1       | Hinge Requirement                                | Required       | Not required                  |
| 2       | Self-Locking                                     | Self-Locking   | Self-Locking but not reliable |
| 3       | Design Flexibility                               | Flexible       | Not much flexible             |
| 4       | Manufacturing                                    | Easy           | Difficult                     |
| 5       | Oscillation Damping at the end of the deployment | Easy           | Difficult                     |
| 6       | Behaviour  | Linear         | Non-Linear                    |

One of the advantages the torsion spring provides is the freedom to choose the number of turns, wire diameter

and coil diameter so as to meet the desired spring stiffness requirement, thus it provides more design flexibility as compared to tape spring.

Oscillations in space are a very well-known problem. Most of them come from orbital features, as the eccentricity of the orbit, the orbit plane, frequency parameters, the true anomaly and moments acting in the satellite axes [1]. The main defect of the traditional deployment mechanisms for solar panels in CubeSats is the lack of position system to block the back-driving of the panel when it reaches the final phase of the deployment [1]. This generates spurious oscillations in the panel, affecting the photovoltaic process as well as generating fatigue in the mechanical elements of the mechanism (hinge or pin) [1]. In COEPSAT-2 the planes of solar panels and solar sail in deployed position are parallel to and around 50 mm apart from each other. The rotation of panels from deployed position towards the sail can damage it and to prevent the damage the rotation angle of panels from deployed position towards sail side is limited to  $10^\circ - 13^\circ$ . This necessitated a stiff and reliable locking mechanism for the mission. The mechanism used in COEPSAT-2 provides deployment and locking as well and is very suitable for other nanosatellites as well due to its simplicity and reliability.

The COEPSAT-2 has four deployable solar panels made of aluminium T6-6061, each having dimensions 260 mm \* 160 mm \* 1 mm and nine solar cells, thus there are a total of thirty-six solar cells being used to suffice the power budget of the satellite. The deployment mechanism has been modelled as a torsional spring mass system with friction damping, having a coefficient of friction of 0.25 (for ABS plastic). The material for torsion spring is high tensile strength stainless steel having Yield Strength of 1700 MPa. The torque needed for smooth deployment ( $t \geq 1$  sec) has been found to be 135 Nmm.

## 2. Theory and calculation

In general, a solar panel deployment process involves three stages viz. (i) Release (ii) Deployment and (iii) Locking. The solar panels are kept in the stowed position using a nylon-nichrome mechanism; to initiate the deployment, current is passed through the nichrome wire resulting in its temperature rise above the melting temperature of the nylon wire touching it. Once the nylon wire gets melted the panel is deployed due to the torque exerted by torsion spring on it and at the same time the locking mechanism gets activated locking the panel in its deployed position.

When the panel is in the un-deployed position, the follower as shown in figure 3.2 exerts an upward force on the cam and it has been found after experimental testing that to provide a reliable locking the required magnitude of this force is around 40 N to 50 N. This generates the friction between the contact surfaces of the

cam and follower as well as between the inner cylindrical surfaces of the hinge and the axle. Thus, the deployment mechanism has been idealised as a torsional spring mass friction damper (Coulomb damping) system to calculate the torque required.

### 2.1 Deployment mechanism

The deployment mechanism utilizes a  $180^\circ$  outside stop hinge loaded with a  $180^\circ$  torsion spring (Fig 1). One leaf of the hinge is fixed on the upper face of the satellite and the other holds the solar panel with the help of screwed fasteners. When the release mechanism is

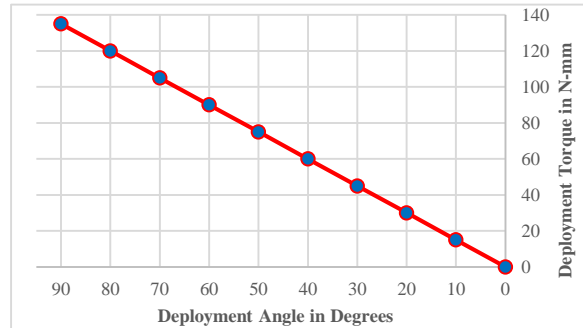


Fig.2. Deployment Angle vs. Deployment Torque  
activated, the strain energy stored in the torsion spring causes the deployment of the solar panel. The torque exerted by the torsion spring on the panel decreases linearly as the deployment proceeds and becomes zero at the end of the deployment (Fig.2.) providing a jerk free deployment of the panel.

### 2.2 Locking Mechanism

The locking mechanism consists of a radial slotted disc cam and a flat spring loaded follower which rests on the outer curved surface of the cam in un-deployed position (Fig.3.2) and fits in the radial slot when it is in the locked or deployed position (Fig.3.3).

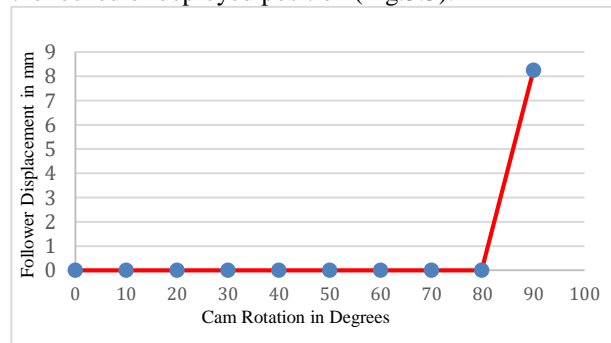


Fig.3.1. Cam Rotation vs. Follower Displacement  
When the deployment angle reaches a value of about  $80^\circ$  the cam follower starts to enter in the slot of the cam and locking is completed when the deployment angle is  $90^\circ$ ; the follower displacement vs. cam rotation graph (Fig 2) is linear during the locking due to the linear profile of the follower tapered face. Locking in the direction opposite to that provided by the cam-follower locking has been

ensured by the projections provided on the panel leaf (Fig.4.).

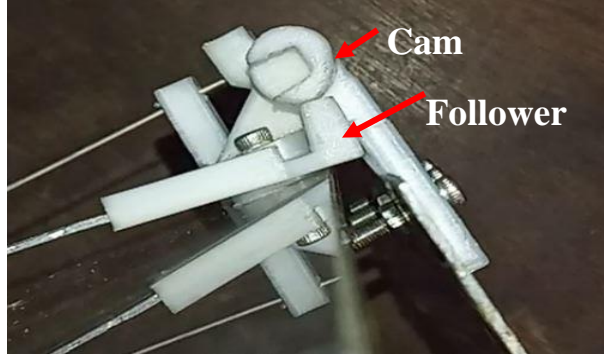


Fig.3.2. Cam-Follower un-locked state

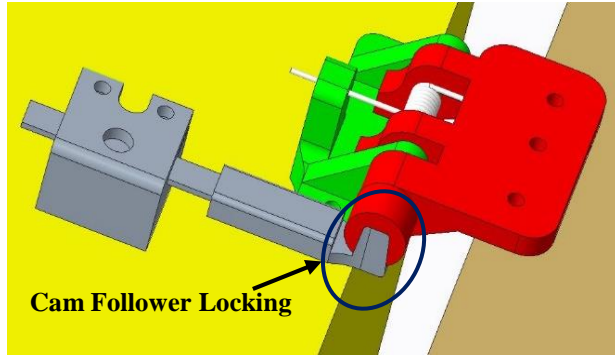


Fig.3.3 Cam-Follower in Locked Position

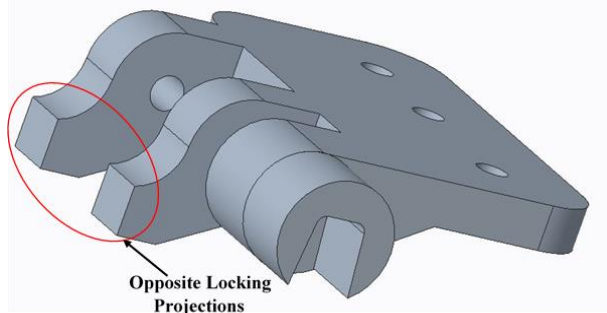


Fig.4. Projections for the locking in opposite direction

### 2.1 Torque required for smooth deployment

An approximate value of torque required for deployment considering the deployment time to be one second and neglecting friction has been calculated as below:

Applying Newton's second law to a rotational system, we have:

$$T = I\ddot{\theta} \quad (1)$$

For the present solar panel:

$$I = \frac{m_{panel} \cdot l_{panel}^3}{3} \quad (2)$$

$$I = \frac{0.132 \times 260^3}{3 \times 1000}$$

$$I = 773.34 \text{ kgm}^4$$

Now,

$$\theta = \frac{1}{2} \cdot \ddot{\theta} \cdot t^2 \quad (3)$$

Taking  $\theta = 90^\circ$  and  $t = 1 \text{ sec}$

We have from equation (3),

$$\ddot{\theta} = 3.14 \text{ rad/sec}^2$$

Therefore, from equation (1),

$$T = 2428.3 \text{ Nm}$$

$$T = 2.4 \text{ Nmm}$$

As this value is obtained by neglecting the friction, the actual value must be greater than this and can't be calculated without knowing the value of frictional torque. On the other hand, to know the value of resisting frictional torque the value of locking force is needed and which can't be known without a preliminary testing. Thus, for testing purpose five torsion spring of different stiffness have been designed and manufactured and the deployment testing has been carried out for each spring.

During the deployment tests it has been found that the reliability of locking depends on the friction between the mutually contacting faces of cam and follower; more is the friction more is the resistance to follower for entering into the cam and once it enters into the cam it gets fitted there and doesn't come out of it due to friction. This frictional resistance is overcome by the locking force provided by the flat spring. The value of locking force depends on the dimensions and material of flat spring; it is directly proportional to width and thickness whereas varies inversely with respect to length. In the present case the value of locking force is restricted due to constraints imposed on the value of width due to space limitations.

For the calculation of actual torque needed for deployment after getting the knowledge of locking force the deployment mechanism has been modelled as a torsional spring mass damper system. Now, from Newton's second law applied to a rotational system the equation of motion for the torsional spring mass friction damper system comes to be as follows:

$$I\ddot{\theta} + \mu N + k\theta = 0 \quad (4)$$

The relation between the number of half cycles after the system comes to rest, friction torque and stiffness is given by equation (5)

$$r \geq \left[ \frac{\theta_0 - \frac{T_f}{k_t}}{\frac{2 \times T_f}{k_t}} \right] \quad (5)$$

$$\text{Now, } \theta_0 = \left( \frac{\pi}{2} \right)^c$$

$$\text{Also, } T = \mu \cdot F_N \cdot R_{cam} \quad (6)$$

$$\therefore T = 0.25 \times 45 \times 6$$

$$= 67.5 \text{ Nmm}$$

The number of half cycles which will cause no oscillation is  $\frac{1}{2}$ . Putting the values of  $\theta_0$  and  $T$  in equation 5 value of  $k_t$  is found to be 85.94 *Nmm/rad* i.e. 1.5 *Nmm/degree*. Hence the initial torque exerted by the spring on the panel is  $1.5 \times 90 = 135 \text{ Nmm}$ .

## 2.2 Design of components using analytical calculations

The components torsion spring, flat spring, cam, follower and leaves of the hinge have been designed analytically by making some reasonable idealisations.

### 2.2.1 Design of Torsion Spring

The torsion spring wire is subjected to bending stresses, hence it is designed considering the tensile strength of the spring wire. The material for spring should have high tensile strength even at elevated temperatures. The material chosen for the spring is high tensile strength stainless steel having tensile strength 1700 MPa. Value of stiffness has been obtained from equation No.2 also, the stiffness of a torsion spring is given by equation No.7

$$k_t = \left( \frac{E_{\text{torsion}} \cdot d^4}{64DN} \right) \quad (7)$$

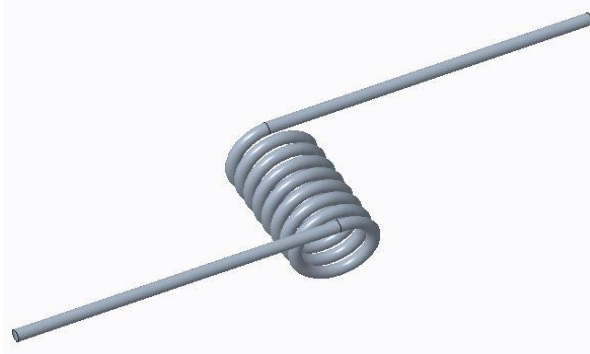


Fig.5. Torsion Spring

The bending stress induced in the torsion spring is given by

$$\sigma_b = K \left( \frac{32T}{\pi d^3} \right) \quad (8)$$

The stress concentration factors for inner fibres is given by

$$K_i = \frac{4C^2 - C - 1}{4C(C-1)} \quad (9)$$

and for outer fibres

$$K_o = \frac{4C^2 + C + 1}{4C(C+1)} \quad (10)$$

Where,

$$C = \frac{D}{d} \quad (11)$$

Stiffness is the function of many variables and hence the design of the torsion spring has been done by trial and error method and imposing the constraints on wire

diameter and length of the spring. The allowable length of spring was around 12 mm and the minimum allowable inner diameter of coil was 2 mm while the maximum coil diameter was limited to 10-12 mm, thus by varying the wire diameter, number of turns and mean coil diameter for different available materials the torsion spring has been designed.

### 2.2.2 Design of Flat Spring

The maximum allowable deflection of the follower owing to height constraints of the satellite is around 8 mm to 9 mm. The flat spring for the follower has been modelled as a cantilever beam with UDL between the ends and having a known deflection at the free end (Fig.

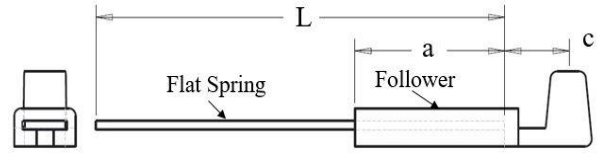


Fig.6. Flat Spring and Follower Assembly

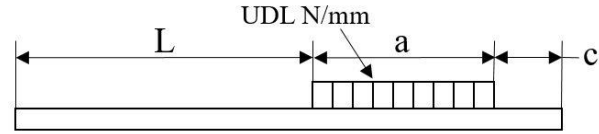
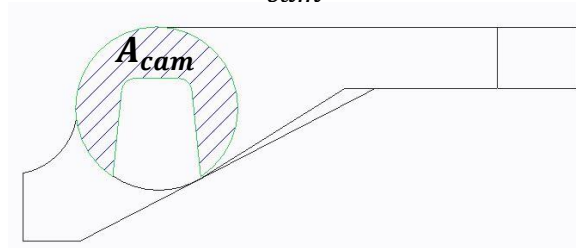


Fig.7. UDL acting on the flat spring due to deflection at free end

### 2.2.3 Design of Panel Fixture

The most critical portion in the panel fixture is cam and is subjected to upward force due to follower in undeployed state. The shear stress induced due to the locking force is found from the equation No.12.

$$\tau_{cam} = \frac{F_N}{A_{cam}} \quad (12)$$



$$A_{cam} = 68 \text{ mm}^2$$

$$\therefore \tau_{cam} = \frac{45}{68} = 0.66 \text{ N/mm}^2$$

The stress value is much below the permissible limit which indicates that the design is safe in shear.

## 3. Results and Discussion

The value of torque required for smooth deployment has been found to be 135 *Nmm* and has been verified experimentally. The stiffness of the torsion spring required for this purpose is thus 1.5 *Nmm/degree*. The



maximum value of the locking force the system can provide is 40 N to 50 N and has been limited due to the space constraints on the upper face of the satellite.

As the flat spring is made of composite (CFRP) and is under a constant deflection which might lead to the stress relaxation and permanent deformation causing unreliable locking; but the extent to which stress relaxation will take place has to be explored before considering this as the limitation of the mechanism.

#### 4. Conclusions

For the mechanism presented, a little consideration will show that it can be used for almost any kind of Pico or Nano satellite due to its simplicity and reliability. Due to the high tensile strength and high elastic modulus of the composites a sufficient locking force has been obtained leading to a more reliable locking and high factor safety.

Also, it should be noted that the main focus of the locking mechanism was to prevent the sail damage due to hitting of solar panel to it and hence more the factor of safety lesser are the chances of sail damage due to the solar panels.

#### Acknowledgements

I would like to give my acknowledgement to Dr. M. P. Khond (Faculty advisor COEP Satellite Team), Dr. M. Y. Khaladkar (Dept. of Applied Sciences College of Engineering, Pune) for their continuous guidance throughout this work. I am also thankful to institute for providing me with the facilities to carry out this work.

#### References

- [1] Arturo Solís-Santome, Guillermo Urriolagoitia-Sosa et al, Conceptual design and finite element method validation of a new type of self-locking hinge for deployable CubeSat solar panels, *Advances in Mechanical Engineering*-January 2019, Vol. 11(1) 1–13
- [2] M. G. El-Sherbiny et al, Design of the Deployment Mechanism of Solar Array on a Small Satellite, *American Journal of Mechanical Engineering*, 2013, Vol. 1, No. 3, 66-72
- [3] Mark Ferris, Andrew Haslehurst, The Use, Evolution and Lessons Learnt of Deployable Static Solar Array Mechanisms, *Proceedings of the 42nd Aerospace Mechanisms Symposium*, NASA Goddard Space Flight Center, May 14-16, 2014
- [4] Tyler Murphy et al, PEZ: Expanding CubeSat Capabilities through Innovative Mechanism Design, 25<sup>th</sup> AIAA/USU Conference on Small Satellites, SSC11-XII-5
- [5] Rachel Trabert et al, The eXtensible Solar Array System: A Modular Nanosatellite Power System, *AIAA/AAS Astrodynamics Specialist Conference* 2–5 August 2010, Toronto, Ontario Canada, AIAA 2010-7654
- [6] Fabio Santoni et al, An innovative deployable solar panel system for Cubesats, *Acta Astronautica* 95(2014)210–217
- [7] Fabio Santoni et al, An orientable solar panel system for nanospacecraft, *Acta Astronautica* 101(2014)120–128
- [8] Patrik Hoan, Design, Construction and Validation of an articulated solar panels for CubeSats, Lulea University of Technology, Master Thesis, Continuation Courses, Space Science and Technology, Department of Space Science, Kiruna
- [9] Tae-Yong Park et al, Development of 6 U CubeSat's Deployable Solar Panel with Burn Wire Triggering Holding and Release Mechanism, *International Journal of Aerospace Engineering* Volume 2019, Article ID 7346436, 13 pages
- [10] Mohammed Chessab Mahdi et al, New Deployable Solar Panel Array for 1u Nanosatellites, *ARPJ Journal of Engineering and Applied Sciences*, vol. 9, no. 11, November 2014
- [11] Jose Miguel Encinas Plaza, Xatcobeo: Small Mechanisms for CubeSat Satellites–Antenna and Solar Array Deployment, *Proceedings of the 40th Aerospace Mechanisms Symposium*, NASA Kennedy Space Center, May 12-14, 2010
- [12] Craig Clark, Huge Power Demand...Itsy-Bitsy Satellite: Solving the CubeSat Power Paradox, 24th AIAA/USU Conference on Small Satellites, SSC10-III-5
- [13] Hamza Baig, Integrated Design of Solar Panels Deployment Mechanism for a Three Unit CubeSat, *American Institute of Aeronautics and Astronautics*, Inc.
- [14] Thomas McGuire, A CubeSat deployable solar panel system, *Energy Harvesting and Storage: Materials, Devices, and Applications VII*; 98650C (2016), Volume 9865